Geomechanics and Engineering, *Vol. 29, No. 1 (2022) 1-11*
https://doi.org/10.12989/gae.2022.29.1.001

Spherical cavity expansion in overconsolidated unsaturated soil under constant suction condition

Hui Wang[a], Changyi Yang* and Jingpei Li[b]

Department of Civil Engineering, Tongji University, Shanghai 200092, China

(Received August 7, 2021, Revised February 8, 2022, Accepted February 11, 2022)

Abstract. A semi-analytical solution to responses of overconsolidated (OC) unsaturated soils surrounding an expanding spherical cavity under constant suction condition is presented. To capture the elastoplastic hydro-mechanical property of OC unsaturated soils, the unified hardening (UH) model for OC unsaturated soil is adopted in corporation with a soil-water characteristic curve (SWCC) and two suction yield surfaces. Taking the specific volume, radial stress, tangential stress and degree of saturation as the four basic unknowns, the problem investigated is formulated by solving a set of first-order ordinary differential equations with the help of an auxiliary variable and an iterative algorithm. The present solution is validated by comparing with available solution based on the modified Cam Clay (MCC) model. Parametric studies reveal that the hydraulic and mechanical responses of spherical cavity expanding in unsaturated soils are not only coupled, but also affected by suction and overconsolidation ratio (OCR) significantly. More importantly, whether hydraulic yield will occur or not depends only on the initial relationship between suction yield stress and suction. The presented solution can be used for calibration of some in-situ tests in OC unsaturated soil.

Keywords: cavity expansion; hydro-mechanical responses; overconsolidated unsaturated soil; suction

1. Introduction

The cavity expansion theory and its applications in saturated soils (Palmer 1972, Mayne 1991, Bolton and Whittle 1999, Charlez and Roatesi 1999, Cudmani and Osinov 2001, Hoek 2001, Frydman 2011, Fahimifar *et al*. 2015, Diao *et al*. 2015, Rezania *et al.* 2017, Agaiby and Mayne 2018, Liu *et al*. 2020, Chen and Zhang 2022) have received significant development in recent decades in terms of proposing new solution techniques (Collins and Stimpson 1994, Chen and Abousleiman 2012, Chen and Abousleiman 2013) and applying various constitutive models (Carter *et al*. 1986, Salgado and Randolph 2001, Collins *et al*. 1992, Silvestri and Abou-Samra 2012, Lukic *et al.* 2014, Vrakas 2016, Sivasithamparam and Castro 2018, Zou *et al.* 2019, Li and Zou 2019, Yang *et al*. 2020, Chen and Mo 2022, Chen *et al*. 2022).

In contrast to the well-developed expansion solutions in saturated soils, only a few types of research have concentrated on cavity expansion in unsaturated soils. The preliminary investigation about cavity expanding in unsaturated sands (Russell and Khalili 2004) showed that expansion responses in saturated and unsaturated sandy soils were substantially different, while the solution technique pertaining to clayey soils was not given. Hence, it is necessary to develop new solutions for cavity expansion in unsaturated clay to eliminate the possible discrepancies induced by applying constitutive models of saturated soil (e.g., modified Cam Clay model). Therefore, with the similarity technique and a unified bounding surface plasticity model for unsaturated soils, Russell and Khalili (2006) presented an analytical solution to expansion responses in unsaturated soils of cavity and emphasized the pressure needed to expand the cavity in unsaturated soil is larger than that in saturated soil. However, only the mechanical responses were modelled without consideration of the irreversible change in degree of saturation, that is, the hydraulic responses in the cavity expansion process. Afterwards, Yang and Russell (2015) developed a solution aimed at the impacts of hydraulic hysteresis on cavity expansion responses in unsaturated silty sand by incorporating a SWCC, and they extended the traditional drained and undrained condition in saturated soils to three generalized drainage conditions in unsaturated soils. It was indicated that the hydraulic behaviour has a significant impact on expansion responses. More recently, Cheng *et al.* (2018) presented a pinpointed solution to cavity expansion responses in finite unsaturated soils to provide possible guidance for experiments in a confined laboratory environment. However, it has to be pointed out that the above solutions to cavity expansion in unsaturated soils do not take the effect of vertical stress into account, because all of them are formulated with simplified mean effective stress and deviator stress. Yang *et al.* (2021) fill this gap by using the elastoplastic critical state model proposed by Sun *et al.* (2008) for unsaturated soils. Both the mean and deviatoric stresses are rigorously defined to derive a solution to

*Corresponding author, Mr.
E-mail: yangcy98@tongji.edu.cn
[a]Mr.
E-mail: wanghui97@tongji.edu.cn
[b]Professor
E-mail: lijp2773@tongji.edu.cn

ISSN: 2005-307X (Print), 2092-6219 (Online)

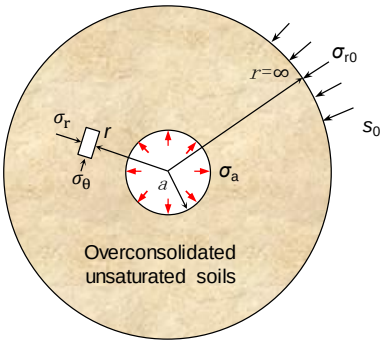

Fig. 1 Schematic of cylindrical cavity expansion in unsaturated soils

expansion responses in unsaturated soil of cylindrical cavity under drained and undrained conditions. Despite these progresses, none of the available solutions takes the hydraulic behaviour as an elastoplastic process. Therefore, the elastoplastic solution to cavity expansion considering both hydraulic hysteresis and hydraulic yield is not available yet.

In this study, an elastoplastic solution to responses of unsaturated soils surrounding an expanding spherical cavity under constant suction condition is presented with consideration of both hydraulic hysteresis and hydraulic yield. The constant suction condition corresponds to sites with good drainage conditions and constant suction test of unsaturated soil in the laboratory environment. The UH model for unsaturated soil (Yao *et al.* 2014) is modified by incorporating a SWCC and two suction yield surfaces (Sun *et al*. 2008) to consider the unique elastoplastic hydro-mechanical property of unsaturated soil. In virtue of an auxiliary variable (Chen and Abousleiman 2013), the problem investigated herein can finally be expressed as a set of first-order ordinary differential equations.

The advantages and significance of the present solution over the existing solutions lie in that: 1) the solution is more general than other solutions due to the adaptation of the UH model for unsaturated soils, which can properly describe the unique responses of OC unsaturated soils surrounding the expanding cavity; 2) both hydraulic hysteresis and hydraulic yield are taken into account in the expansion process, which is non-trivial and induces significant complication in formulation; 3) an advanced iterative computational method is employed to solve the coupled hydro-mechanical constitutive matrix in particular.

The proposed solution is calibrated and compared with the results of UH model-based solution and MCC model-based solution (Rao *et al*. 2017) to highlight the impacts of coupled hydro-mechanical behaviour on cavity expansion responses and the advances of employing UH model for unsaturated soils.

2. Definition of the problem

The problem investigated is about a spherical cavity expanding in infinite homogeneous unsaturated and OC soil under drained condition, which is taken as a premise that the suction stay constant. The in-situ stresses include the net stress σ_{r0} and suction s_0, as shown in Fig. 1.

During the expansion process, as the internal expanding pressure increases from its initial value of σ_0 to the current pressure σ_a, the cavity radius increases from a_0 to a. Meanwhile, a material particle will move outwards from the initial radial position r_0 to the current position r, and the corresponding radial displacement of which is denoted by U_r. It should be emphasized that although the deformation is comparatively small in the far field, plastic strain occurs inextricably in OC soils once the loading commences. Hence, it is assumed to be no pure-elastic region and only one elastoplastic region that extends to infinity surrounding the cavity. Furthermore, there are another two points that should be noted as follows: (a) The compressive stress and strain involved in the formulations are regarded to be positive as a convention adopted in soil mechanics; (b) Since the spherical cavity is subjected to hydrostatic pressure, the expansion problem is modelled as plane strain process.

In the spherical coordinates, the equilibrium equation of a typical soil unit at the radial position r can be expressed as

$$\frac{\mathrm{d}\sigma_r}{\mathrm{d}r}+2\frac{\sigma_r-\sigma_\theta}{r}=0 \tag{1}$$

where the symbol 'd()' represents the differential and derivative described in Eulerian description; σ_r and σ_θ denote radial and circumferential net stresses, respectively.

Owing to the self-similar and symmetry properties of the spherical cavity expansion problem, the problem investigated can be finally expressed as a set of differential equations based on the Lagrangian description, which is not within the same framework of the equilibrium equation. Therefore, in order to facilitate the conversion between these two schemes, the equilibrium equation can be transformed to the expression within Lagrangian description by employing an auxiliary variable ξ as

$$\frac{\mathrm{D}\sigma_r}{\mathrm{D}\xi}\frac{\mathrm{d}\xi}{\mathrm{d}r}+2\frac{\sigma_r-\sigma_\theta}{r}=0 \tag{2}$$

$$\xi=\frac{U_r}{r}=\frac{r-r_0}{r} \tag{3}$$

where symbol 'D()' means the differential and derivative regarding the Lagrangian description; ξ is an auxiliary variable proposed by Chen and Abousleiman (2013); and the spatial derivative of U_r with respect to the radial position can be expressed as (Rao *et al.* 2017)

$$\frac{\mathrm{d}U_r}{\mathrm{d}r}=1-\frac{v_0}{v(1-\xi)^2} \tag{4}$$

in which v and v_0 are current and initial specific volume, respectively.

3. Coupled hydro-mechanical model for spherical cavity expansion

To consider the elastoplastic hydro-mechanical behaviours of unsaturated soils, the UH model for unsaturated soil (Yao *et al.* 2014) is adopted in corporation

with a SWCC and two suction yield surfaces (Sun *et al*. 2008). The reason for this modification is that the UH model for unsaturated soil only models the mechanical responses of unsaturated soils (i.e., the variations of suction and net stress) while ignoring the significant hydraulic responses of unsaturated soils (i.e., the change of degree of saturation). Due to the specific volume generally acts as a basic parameter in cavity expansion problem, a SWCC related to the void ratio proposed by Sun *et al*. (2008) is adopted, which can properly reflect the irreversible change of degree of saturation. To facilitate the following formulation, some basic properties of the SWCC revised constitutive model are briefly reviewed herein.

3.1 UH model for overconsolidated unsaturated soil

The UH model for unsaturated soil consists of two yield surfaces in the $p-q$ plane: the current and the reference yield surfaces, and the geometric relationship between the two yield surfaces shown in Fig. 2 can reflect the effects of stress history and overconsolidation degree. The mechanical behavior of unsaturated soil is governed by current yield function and the associated flow rule, which is given by

$$f(p,q,s,H)=q^2-M^2(p+p_\mathrm{s})(p_\mathrm{x}-p)=0 \tag{5}$$

where M is the characteristic state stress ratio; p and q are the mean net stress and the deviator net stress, which are defined as

$$p=\frac{1}{3}\sigma_{ij}\delta_{ij} \tag{6}$$

$$q=\sqrt{\frac{3}{2}s_{ij}s_{ij}} \tag{7}$$

$$s_{ij}=\sigma_{ij}-p\delta_{ij} \tag{8}$$

where δ_{ij} is the Kronecker delta; $p_\mathrm{s}=ks$ is the value of the left intersection of current yield surface and $p-$axis under a known suction s, and k is a material constant; p_x is the mean net stress at the right intersection of current yield surface and $p-$axis under a known suction s, and it can be obtained by load-collapse (LC) yield curve in the $p-s$ plane as

$$p_\mathrm{x}=p^\mathrm{c}\left(\frac{p_\mathrm{x}^*}{p^\mathrm{c}}\right)^{\frac{\lambda(0)-\kappa}{\lambda(s)-\kappa}} \tag{9}$$

where p_x^* is the mean net stress at the right intersection of yield surface and p-axis for saturated soil; p^c is a reference stress; κ is the slope of unloading line for unsaturated soil; $\lambda(s)$ and $\lambda(0)$ are the slopes of the normal compression lines of unsaturated soil with suction s and saturated soil in the $e-\ln p$ plane, respectively.

Instead of adopting the volumetric strain as the hardening parameter, the hardening law of the UH model for unsaturated soil is based on p_x^* and the well-known unified hardening parameter H as

$$c_\mathrm{p}\mathrm{D}(\ln p_\mathrm{x}^*)=c_\mathrm{p}\frac{\mathrm{D}p_\mathrm{x}^*}{p_\mathrm{x}^*}=\mathrm{D}H=\frac{1}{\Omega}\mathrm{D}\varepsilon_\mathrm{v}^\mathrm{p} \tag{10}$$

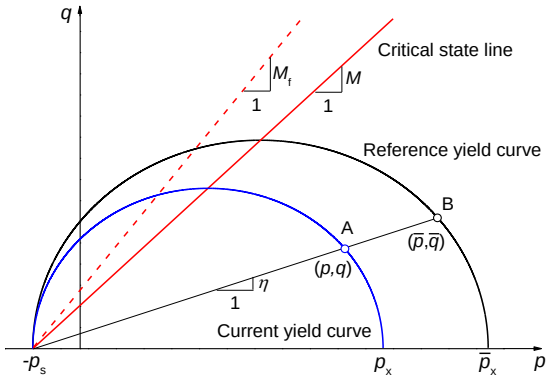

Fig. 2 Current yield surface and reference yield surface

where $\varepsilon_\mathrm{v}^\mathrm{p}$ is the plastic volumetric strain; c_p and Ω are the abbreviations for the following mathematical expressions

$$c_\mathrm{p}=\frac{\lambda(0)-\kappa}{1+e_0} \tag{11}$$

$$\Omega=\frac{M^4-\eta^4}{M_\mathrm{f}^4-\eta^4} \tag{12}$$

in which $\eta=q/(p+p_\mathrm{s})$ is the stress ratio for unsaturated soils; e_0 is the initial void ratio; M_f is the potential failure stress ratio, which can be further related to M and the OC parameter R as

$$M_\mathrm{f}=\sqrt{\frac{3M^2}{R(3-M)}\left[1+\frac{M^2}{12R(3-M)}\right]}-\frac{M^2}{2R(3-M)} \tag{13}$$

It is instructive to indicate that there is a difference between OC parameter R and the overconsolidation ratio (OCR). Because the OCR is generally a constant in classical constitutive models (e.g., the MCC model and Barcelona basic model), but the OC parameter in UH model for unsaturated soil evolves with the mechanical and hydraulic state of soils around the cavity during the expansion process, which can be expressed as (Yao *et al.* 2014)

$$R=\frac{(p+p_\mathrm{s})(1+\frac{\eta^2}{M^2})}{\bar{p}_{\mathrm{x}0}\exp\left[\frac{\lambda(0)-\kappa}{\lambda(s)-\kappa}\frac{\varepsilon_\mathrm{v}^\mathrm{p}}{c_\mathrm{p}}\right]+p_\mathrm{s}} \tag{14}$$

where $\bar{p}_{\mathrm{x}0}$ is the initial value of the right intersection of reference yield surface and $p-$axis under a certain suction.

3.2 Soil-water characteristic behaviour of unsaturated soil

The relationship between the two hydraulic parameters suction s and the degree of saturation S_r can be represented by the main drying/wetting curve and scanning curve as shown in Fig. 3, which can be expressed as (Sun *et al.* 2008)

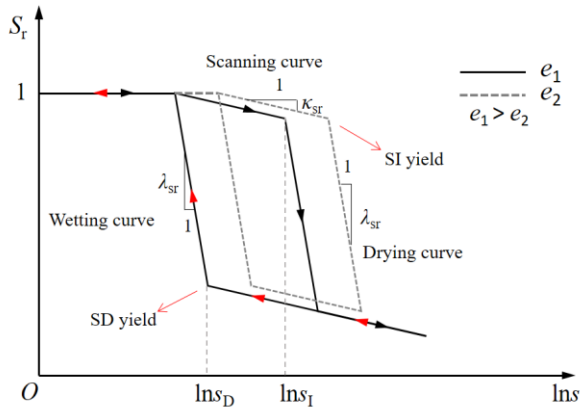

Fig. 3 Void ratio-dependent soil-water characteristic curve

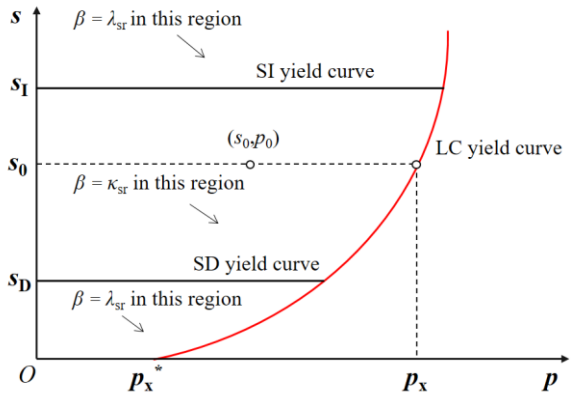

Fig. 4 Mechanical and hydraulic yield curves in p-s plane

$$\mathrm{D}S_r = -\lambda_{se}\mathrm{D}e - \beta\frac{\mathrm{D}s}{s} \tag{15}$$

where λ_{se} is the slope of the $S_r - e$ curve under constant suction; β is a unified parameter to express the SWCC; if the hydraulic state is on the main curve, $\beta = \lambda_{sr}$ (the slope of the main drying/wetting curve); otherwise $\beta = \kappa_{sr}$ (the slope of the scanning curve), which denotes that the hydraulic state is on the scanning curve.

Apart from mechanical yielding, unsaturated soils also yield owing to changes of hydraulic change as shown in Fig. 4. The hydraulic yielding, which generally corresponds to the transition between the main curve and scanning curve, is assumed to be governed by the suction increase (SI) yield curve and suction decrease (SD) yield curve in the $p - s$ plane as

$$f_{SI} = s - s_I = 0 \tag{16}$$

$$f_{SD} = s_D - s = 0 \tag{17}$$

where s_I and s_D are SI and SD yield stresses, respectively.

If $s > s_I$ or $s_0 < s_D$, the hydraulic state yields; otherwise, the hydraulic state remain elastic. Therefore, along with the LC yield curve, the two suction yield curves can guarantee that both the hydraulic and mechanical responses of unsaturated soils are modelled as an elastoplastic process.

It has been emphasized that the SWCC is a void ratio-dependent one as shown in the solid and dashed lines in Fig. 3. Therefore, as the specific volume of unsaturated soils around the cavity evolves during the expansion of the cavity, the yield values of SI and SD yield curves should also depend on void ratio. To identity the current hydraulic state, it is important to obtain the evolution law of s_I and s_D during the expansion process.

As shown in Fig. 5, the initial SD yield point locates at A_0 $(S_{r0}, \ln s_{D0})$, where the initial wetting and scanning curves intersect in the $S_r - \ln s$ plane. Extend the wetting and scanning curves, and these two curves will intersect the S_r −axis at $S_{rw}(e_0)$ and $S_{rs}(e_0)$. During the expansion of the cavity, the current SWCC evolves with the change of void ratio as the wetting curve and scanning curve move upward for a distance of ΔS_{rw} and ΔS_{rs}, respectively. Correspondingly, the current SD yield point move to A $(S_r, \ln s_D)$. The initial and current value of the degree of saturation of the SD yield point, S_{r0} and S_r, can be obtained according to the simple geometric relationship as

$$S_{r0} = S_{rw}(e_0) - \lambda_{sr}\ln s_{D0} \tag{18}$$

$$S_r = S_{rw}(e) - \lambda_{sr}\ln s_D = S_{rw}(e_0) + \Delta S_{rw} - \lambda_{sr}\ln s_D \tag{19}$$

where e_0 and e are the initial and current values of void ratio; ΔS_{rw} can be related to the initial and current void ratio as

$$\Delta S_{rw} = -\lambda_{se}(e - e_0) \tag{20}$$

Substituting Eqs. (18) and (20) into Eq. (19), the current value of SD yield s_D can be expressed as

$$s_D = s_{D0}\exp\left[\frac{S_{r0} - S_r - \lambda_{se}(e - e_0)}{\lambda_{sr}}\right] \tag{21}$$

Since the cavity is assumed to expand in unsaturated soil under constant suction condition, integrating Eq. (15) gives

$$S_r = S_{r0} - \lambda_{se}(e - e_0) \tag{22}$$

Substituting Eq. (22) into Eq. (21), the relationship between s_{D0} and s_D can be obtained as

$$s_D = s_{D0} \tag{23}$$

It can be demonstrated from Eq. (23) that the SD yield stress s_D is equal to its initial value s_{D0} constantly throughout the whole expansion process of spherical cavity in unsaturated soils under drained condition. Similarly, it can be proved that the SI yield stress s_I also keeps as a constant during the whole expansion process. It can be concluded that the current hydraulic state is only related to the relationship between the initial values of SI and SD yield stress s_{I0}, s_{D0} and the initial suction s_0. If $s_0 > s_{I0}$ or $s_0 < s_{D0}$, the hydraulic state yields constantly and therefore $\beta = \lambda_{sr}$; if $s_{I0} < s_0 < s_{D0}$, the hydraulic state is on the scanning curve and remains elastic during the whole loading process, and β would be adopted as κ_{sr}.

3.3 Constitutive matrix

The constitutive matrix of spherical cavity expansion in saturated soil has been given by Rao *et al.* (2017), which is

exactly the same as the mechanical part of constitutive matrix of spherical cavity expansion in unsaturated soil. Therefore, the coupled hydro-mechanical constitutive matrix of the problem investigated can be obtained by combining Rao *et al*. (2017) and Eq. (14) as follows

$$\begin{bmatrix} \mathrm{D}\varepsilon_\mathrm{r} \\ \mathrm{D}\varepsilon_\theta \\ \mathrm{D}S_\mathrm{r} + \lambda_\mathrm{se}\mathrm{D}v \end{bmatrix} = \begin{bmatrix} \frac{1}{E} + aa_\mathrm{r}^2 & -\frac{2\mu}{E} + 2aa_\mathrm{r}a_\theta & 0 \\ -\frac{\mu}{E} + aa_\mathrm{r}a_\theta & \frac{1-\mu}{E} + 2aa_\theta^2 & 0 \\ 0 & 0 & -\frac{\beta}{S} \end{bmatrix} \begin{bmatrix} \mathrm{D}\sigma_\mathrm{r} \\ \mathrm{D}\sigma_\theta \\ \mathrm{D}s \end{bmatrix} \tag{24}$$

where μ is Poisson's ratio; E is the elastic modulus pertaining to the net stress change, the detailed definition of which can be found in Yao *et al*. (2014), both μ and E are considered to be constant; $\mathrm{D}\varepsilon_\mathrm{r}$ and $\mathrm{D}\varepsilon_\theta$ are increments of radial and tangential strain; $\mathrm{D}\sigma_\mathrm{r}$ and $\mathrm{D}\sigma_\theta$ are increments of radial and tangential stress; $\mathrm{D}s$ is the increment of suction; a, a_r and a_θ are abbreviations for the following expressions

$$a = -\frac{c_\mathrm{p}\Omega[\lambda(s)-\kappa]}{M^4 p_\mathrm{x}^*(p+p_\mathrm{s})(p_\mathrm{x}-2p-p_\mathrm{s})[\lambda(0)-\kappa]}\left(\frac{p_\mathrm{x}^*}{p^c}\right)^{\frac{\lambda(0)-\lambda(s)}{\lambda(s)-\kappa}} \tag{25}$$

$$a_\mathrm{r} = -\frac{1}{3}M^2(p_\mathrm{x}-2p-p_\mathrm{s}) + 3(\sigma_\mathrm{r}-p) \tag{26}$$

$$a_\theta = -\frac{1}{3}M^2(p_\mathrm{x}-2p-p_\mathrm{s}) + 3(\sigma_\theta-p) \tag{27}$$

Taking inverse calculation of the constitutive matrix (24) and considering that the drained condition for unsaturated soils, constitutive matrix (24) can be written as

$$\begin{bmatrix} \mathrm{D}\sigma_\mathrm{r} \\ \mathrm{D}\sigma_\theta \\ 0 \end{bmatrix} = \begin{bmatrix} b_\mathrm{rr}/\Delta & b_\mathrm{r\theta}/\Delta & 0 \\ b_\mathrm{\theta r}/\Delta & b_\mathrm{\theta\theta}/\Delta & 0 \\ 0 & 0 & -\frac{\beta}{S} \end{bmatrix} \begin{bmatrix} \mathrm{D}\varepsilon_\mathrm{r} \\ \mathrm{D}\varepsilon_\theta \\ \mathrm{D}S_\mathrm{r} + \lambda_\mathrm{se}\mathrm{D}v \end{bmatrix} \tag{28}$$

where $b_\mathrm{rr} = E(2Eaa_\theta^2 + 1 - \mu)$; $b_\mathrm{r\theta} = 2E(\mu - Eaa_\mathrm{r}a_\theta)$; $b_\mathrm{\theta r} = E(\mu - Eaa_\mathrm{r}a_\theta)$; $b_\mathrm{\theta\theta} = E(Eaa_\mathrm{r}^2 + 1)$; and $\Delta = (1-\mu)Eaa_\mathrm{r}^2 + 4\mu Eaa_\mathrm{r}a_\theta + 2Eaa_\theta^2 + 1 - \mu - 2\mu^2$.

3.4 Governing equations of spherical cavity expansion problem

As for the problem investigated, the relationship among increment of volumetric strain $\mathrm{D}\varepsilon_\mathrm{v}$, increment of radial strain $\mathrm{D}\varepsilon_\mathrm{r}$ and increment of tangential strain $\mathrm{D}\varepsilon_\theta$ can be given as

$$\mathrm{D}\varepsilon_\mathrm{v} = \mathrm{D}\varepsilon_\mathrm{r} + 2\mathrm{D}\varepsilon_\theta \tag{29}$$

where $\mathrm{D}\varepsilon_\mathrm{v}$ and $\mathrm{D}\varepsilon_\mathrm{r}$ can be further expressed based on the large strain theory as

$$\mathrm{D}\varepsilon_\mathrm{v} = \frac{\mathrm{D}v}{v} \tag{30}$$

$$\mathrm{D}\varepsilon_\theta = -\frac{Dr}{r} = -\frac{\mathrm{D}\xi}{1-\xi} \tag{31}$$

Therefore, the expression of $\mathrm{D}\varepsilon_\mathrm{r}$ can be obtained as

$$\mathrm{D}\varepsilon_\mathrm{r} = \mathrm{D}\varepsilon_\mathrm{v} - 2\mathrm{D}\varepsilon_\theta = \frac{\mathrm{D}v}{v} - 2\left(-\frac{Dr}{r}\right) = \frac{\mathrm{D}v}{v} + 2\frac{\mathrm{D}\xi}{1-\xi} \tag{32}$$

Substituting Eqs. (31) and (32) into Eq. (28) gives

$$\frac{\mathrm{D}\sigma_\mathrm{r}}{D\xi} = \frac{1}{\Delta}\left[\frac{2b_\mathrm{rr} - b_\mathrm{r\theta}}{1-\xi} - \frac{\mathrm{D}v}{D\xi}\frac{b_\mathrm{rr}}{v}\right] \tag{33}$$

$$\frac{\mathrm{D}\sigma_\theta}{D\xi} = \frac{1}{\Delta}\left[\frac{2b_\mathrm{\theta r} - b_\mathrm{\theta\theta}}{1-\xi} - \frac{\mathrm{D}v}{D\xi}\frac{b_\mathrm{\theta r}}{v}\right] \tag{34}$$

$$\frac{\mathrm{D}S_\mathrm{r}}{\mathrm{D}\xi} = -\lambda_\mathrm{se}\frac{\mathrm{D}v}{D\xi} \tag{35}$$

Because there are only four unknowns left in Eqs. (33)-(35), the differential equations can be solved in conjunction with equilibrium equation Eq. (2).

The material derivative of σ_r with regard to ξ can be determined by combining the equilibrium equation and the derivative of ξ with regard to r given by Chen and Abousleiman (2013) as

$$\frac{\mathrm{D}\sigma_\mathrm{r}}{\mathrm{D}\xi} = -\frac{2(\sigma_\mathrm{r}-\sigma_\theta)}{1-\xi-\frac{v_0}{v(1-\xi)^2}} \tag{36}$$

Combining Eq. (33) and Eq. (36), the material derivative of v with regard to ξ can be expressed as

$$\frac{\mathrm{D}v}{\mathrm{D}\xi} = \left[\frac{2(\sigma_\mathrm{r}-\sigma_\theta)}{1-\xi-\frac{v_0}{v(1-\xi)^2}} + \frac{2b_\mathrm{rr} - b_\mathrm{r\theta}}{\Delta(1-\xi)}\right]\frac{\Delta v}{b_\mathrm{rr}} \tag{37}$$

Substituting Eq. (37) into Eqs. (34) and (35) gives

$$\frac{\mathrm{D}\sigma_\theta}{D\xi} = -\frac{b_\mathrm{\theta r}}{b_\mathrm{rr}}\left[\frac{2(\sigma_\mathrm{r}-\sigma_\theta)}{1-\xi-\frac{v_0}{v(1-\xi)^2}} + \frac{2b_\mathrm{rr} - b_\mathrm{r\theta}}{\Delta(1-\xi)}\right] + \frac{2b_\mathrm{\theta r} - b_\mathrm{\theta\theta}}{\Delta(1-\xi)} \tag{38}$$

$$\frac{\mathrm{D}S_\mathrm{r}}{\mathrm{D}\xi} = -\lambda_\mathrm{se}\left[\frac{2(\sigma_\mathrm{r}-\sigma_\theta)}{1-\xi-\frac{v_0}{v(1-\xi)^2}} + \frac{2b_\mathrm{rr} - b_\mathrm{r\theta}}{\Delta(1-\xi)}\right]\frac{\Delta v}{b_\mathrm{rr}} \tag{39}$$

Up to now, Eqs. (36)-(39) make up the governing equations for the problem that spherical cavity expanding in OC unsaturated soils, which can be solved with the initial values of the four basic unknowns.

3.5 Initial values and conversion between ξ and r

Since the plastic zone is assumed to be infinite, the initial condition is set at infinity where the radial displacement U_r of a given material particle equals to zero and therefore, ξ_0, the initial value of ξ, also equals to zero. The initial values of the four basic unknowns and suction s at infinity can be determined, respectively, as follows.

$$\sigma_\mathrm{rp} = \sigma_\mathrm{\theta p} = \sigma_0 \tag{40}$$

$$v_{\mathrm{p}} = v_0 \tag{41}$$

$$s_{\mathrm{p}} = s_0 \tag{42}$$

$$S_{\mathrm{rp}} = S_{\mathrm{r0}} \tag{43}$$

It can be found from the governing equations that the solutions will be presented in the form of auxiliary variable ξ. In order to make the solution more clear, it is necessary to transform the auxiliary variable ξ to the actual radial coordinate r, which can be achieved according to Chen and Abousleiman (2013) as

$$\frac{r}{a} = \exp\left(\int_{\xi_{\mathrm{a}}}^{\xi} \frac{v(1-\xi)^2}{v(1-\xi)^3 - v_0}\mathrm{d}\xi\right) \tag{44}$$

where $\xi_{\mathrm{a}} = 1 - a/a_0$ is the auxiliary variable at the cavity wall.

3.6 Solution technique

It is important to point out that the OC parameter R changes during cavity expansion with stress state and specific volume. At the same time, both the two variables are basic unknowns included in the governing equations. Therefore, employing the built-in functions in MATLAB or MATHEMATICA to directly solve the governing equations would be impossible. To fill in this gap, the iterative algorithm proposed by Yang *et al.* (2021) for cylindrical cavity expansion problem is employed and further modified to make it pertaining to the spherical cavity problem. With this algorithm, the value of all parameters can be updated in each step and the governing equations can be readily solved.

4. Results and discussions

In this section, a comprehensive parametric study is carried out to investigate the predominant features of responses of OC unsaturated soils surrounding an expanding spherical cavity. The expansion responses investigated herein involve distributions of specific volume, degree of saturation and two principal stress components around the cavity, the net stress paths, the expansion pressures and the degree of saturation at cavity wall corresponding to different cavity radii.

4.1 Input parameters

A typical soil is employed from Chen and Abousleiman (2013) in the parametric study, and the basic properties of which are listed as $\sigma_0 = 120$ kPa, $v_0 = 2.1$, w_0 = 24.09%, G_{s} = 2.74, M = 1.2, $\lambda(0)$ = 0.15, λ_{se} = 0.21, λ_{sr} = 0.12, κ_{sr} = 0.04, k = 0.6, $p^{\mathrm{c}} = 10$ kPa. The elastic parameters are κ = 0.03 and μ = 0.3. Five sets of OCR (1, 5, 10, 20 and 30) are included to cover normally, moderately OC and heavily OC soil. The initial degree of saturation and suction are set as 0.6 and 90 kPa, respectively.

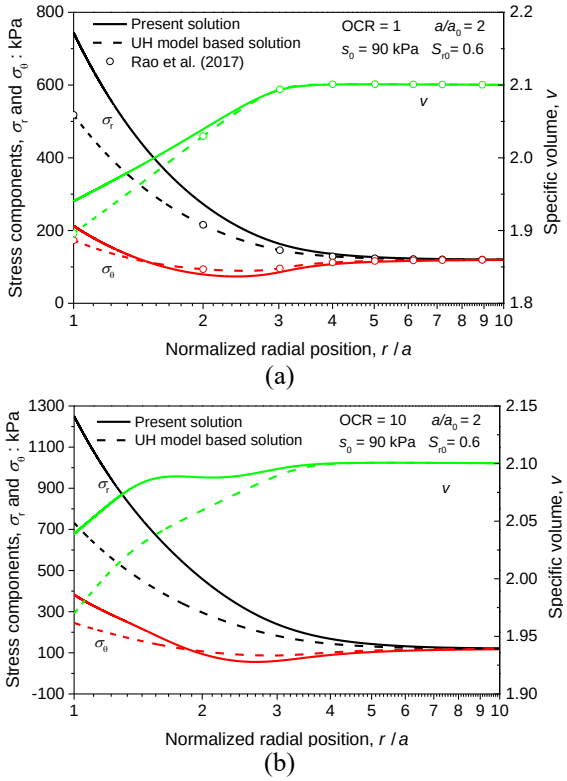

Fig. 6 Comparisons for distribution of stress components and specific volume with other solutions for: (a) OCR=1 and (b) OCR=10

4.2 Expansion responses comparing with other solutions

The UH model-based solution and the MCC model-based solution proposed by Rao *et al.* (2017) for spherical cavity expansion responses in saturated soil under drained condition are adopted as comparisons to explore the influence of coupled hydro-mechanical behavior on cavity expansion responses. Due to the fact that MCC model cannot well describe the unique mechanical behavior of OC soil, the present solution only compares with the MCC model-based solution for NC soil, which also services as a validation of the present solution.

Figs. 6(a) and 6(b) show the distributions of radial net stress σ_{r}, tangential net stress σ_{θ} and specific volume v around the cavity versus the normalized radial position r/a when the expansion ratio $a/a_0 = 2$ for normally consolidated (NC) soil and heavily OC soil with $\mathrm{OCR} = 10$, respectively. Since all the three solutions shown in Fig. 6(a) aim at NC soil and have the same assumption that the soil yields once loading happens, the only difference among the three solutions lies in the suction existed in unsaturated soils rather than the constitutive model. It is apparently shown in Fig. 6(a) that the present solution to expansion responses in NC unsaturated soil of cavity can reduce to the MCC model-based solution to expansion responses in saturated soil perfectly when suction $\mathrm{s} = 0$, which validates the correctness of present solution. It also can be found in Fig. 6(a) that the two principal stress components in unsaturated soil are higher than that in fully saturated soil

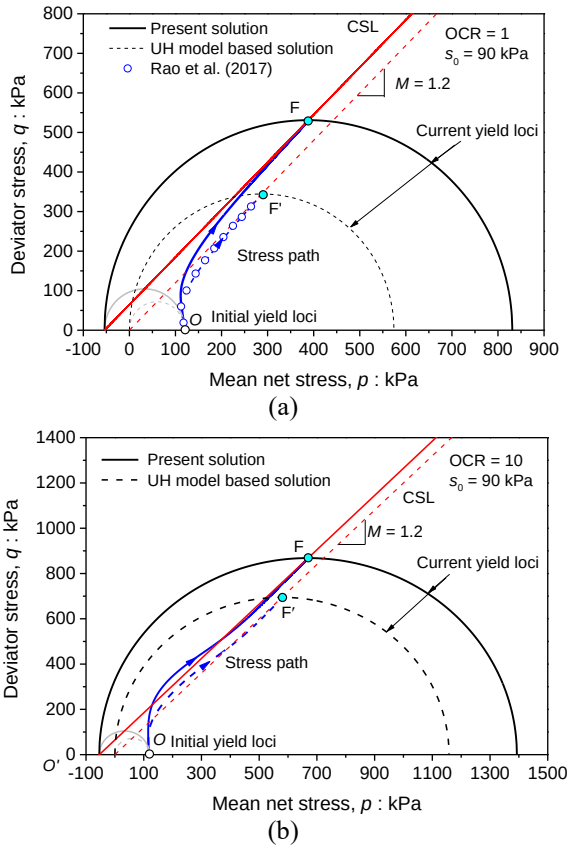

Fig. 7 Comparisons for net stress paths of a soil particle at cavity wall with other solutions for: (a) OCR=1 and (b) OCR=10

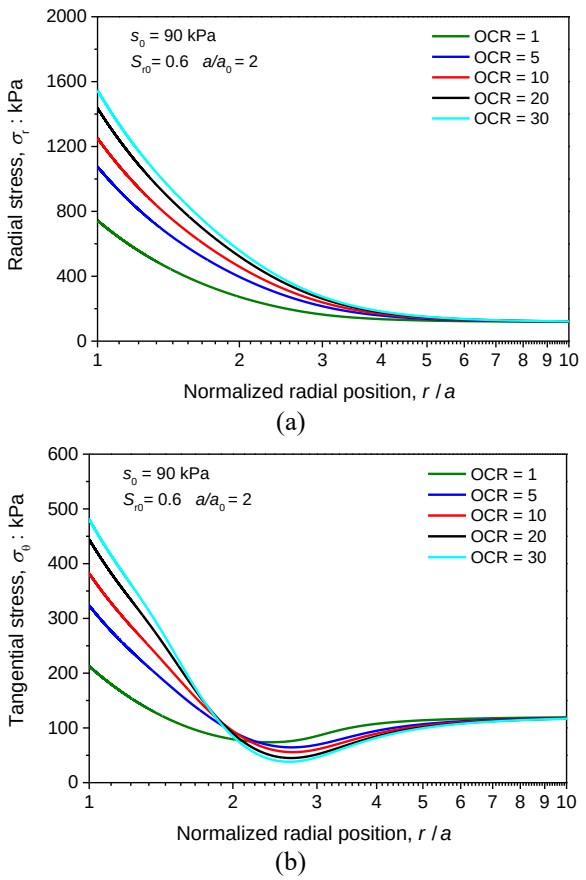

Fig. 8 Distributions of (a) radial stress; and (b) tangential stress around cavity for different OCRs

around the cavity. It is also interesting to find that the changing range of specific volume v around the cavity in unsaturated soil is minor than that in fully saturated soil, which demonstrates that unsaturated soil is more rigid than saturated soil due to the enhancement (Gong *et al*. 2017). Further comparison between Figs. 6(a) and 6(b) reveals that the above phenomenon is even more obvious in heavily OC soil, which means the suction might play a more important role in heavily OC soil than that in NC soil.

Figs. 7(a) and 7(b) plot the net stress paths of a material particle at the cavity wall during cavity expansion process for unsaturated soil with $\mathrm{OCR} = 1$ and $\mathrm{OCR} = 10$ in the $p - q$ plane, respectively. The corresponding initial and current loci are also plotted in Figs. 7(a) and 7(b). The effective stress paths of spherical cavity expansion in saturated soil under drained condition generated by MCC model-based solution and UH model-based solution are also plotted for comparison. As shown in Figs. 7(a) and 7(b), the initial state stress point *O* of the UH model and the UH model for unsaturated soil is located at initial yield loci, which corresponds to the assumption that the material particles at the cavity wall yields instantly once the cavity starts to expand (Zhou *et al*. 2022). It is obvious that the stress paths of NC soil develop from the initial state stress point *O*, then move up and right approaching the critical state line (CSL), and at last reach the current state stress point F (F') where the current yield loci and CSL intersect. However, the stress path in OC soil shown in Fig. 7(b) has different developing trend from that in NC soil. The paths start from the initial state stress point and firstly turn up and slightly right. It seems that the stress path passes through the CSL, and then moves towards upper right and passes over the CSL for a second time rather than terminating at the first intersection with the CSL as NC soil does. This phenomenon can be attributed to that the stress state is actually evolving in a three-dimensional stress space, and the stress increment can be in line with the neutral loading direction, which is vertical to the current yield locus. Since the OC unsaturated soil undergoes plastic hardening, then softening, and finally hardening again during the expansion process, the stress path crosses the CSL twice. The intersection between the stress path and CSL generally corresponds to the transition between volumetric softening and hardening behavior. Although the stress paths of different solution own the similar developing trend, the stress paths of unsaturated soil lie above those of saturated soil, which again indicates the existence of suction increases the strength of unsaturated soil (Zhang *et al.* 2020). In addition, because suction has been considered in the present solution, both the left intersection of yield loci and p −axis and the origin of CSL are at $(-ks, 0)$ rather than $(0, 0)$ as UH model-based solution and MCC model-based solution do. Note that according to the symmetric property of the spherical cavity problem, the stress path in the deviatoric plane is just a straight line, which is therefore not presented herein.

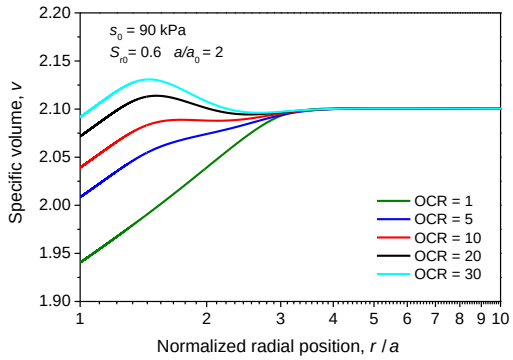

Fig. 9 Distributions of specific volume around cavity for different OCRs

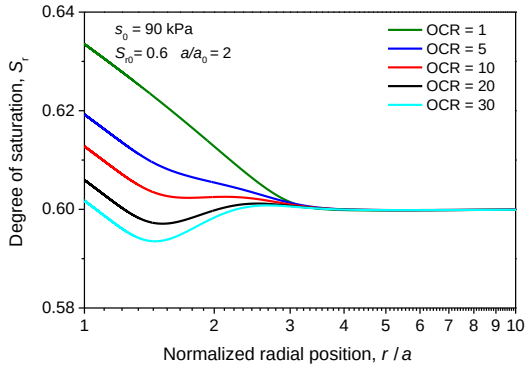

Fig. 10 Distributions of degree of saturation around cavity for different OCRs

4.3 Distribution of basic unknowns around cavity for different OCRs

Distributions of net radial stress σ_r and tangential stress σ_θ around cavity for different OCRs including 1, 5, 10, 20 and 30 as the cavity expands to twice its initial radius are drawn versus normalized radial position r/a in Figs. 8(a) and 8(b), respectively. The radial stress σ_r and tangential stress σ_θ have some similar patterns, such as the value of both the two stress at cavity wall increasing with OCR, which is on account of enhancement of overconsolidation to the strength of unsaturated soil. The differences lie in that the radial stress for all OCRs is monotonically decreasing along with radial position. In contrast, the tangential stress has a different distribution trend of decreasing first and then increasing as the radial position increases.

Distribution of specific volume v around cavity at the moment when $a/a_0 = 2$ is plotted versus normalized radial position r/a in Fig. 9. On the contrary of radial and tangential stresses, the changing range of specific volume around the cavity decreases with OCR, which indicates the soil is more rigid as OCR increases. As shown in Fig. 9, the specific volume of NC soil and moderately OC soil increases with the normalized radial position. However, the specific volume of heavily OC soil shows a different distribution pattern, which increases at first, then decreases until $r/a = 3$ approximately, and at last increases a little again to the initial specific volume.

Similar to the specific volume, Fig. 10 plots the distribution of degree of saturation at the instant $a/a_0 = 2$ for different OCRs, including 1, 5, 10, 20 and 30. The degree of saturation of moderately OC soil and NC soil decreases monotonously along with the normalized radial position. However, owing to the shear dilatancy of heavily OC soils, the degree of saturation of OC soils has a decreasing-increasing-decreasing process. In addition, approximately at the normalized radial position $r/a = 5$, all degree of saturation distribution curves for different OCRs gather to the initial value of degree of saturation. It can be seen from comparisons between Figs. (9) and (10) that the distribution patterns of the specific volume and the degree of saturation are reverse, which can be explained by Eq. (22).

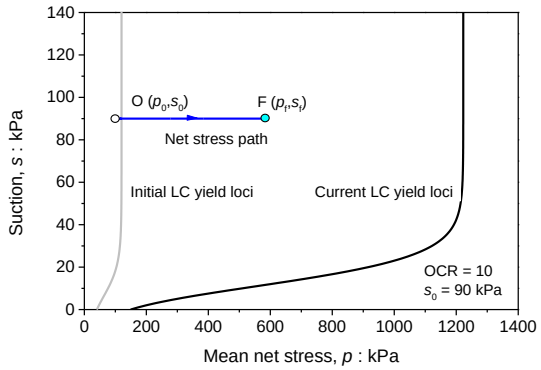

Fig. 11 Projection of net stress paths in $p-s$ plane for OCR=10

4.4 Projection of net stress path in $p-s$ plane

In Fig. 11, the projection of the net stress path is plotted in $p-s$ plane, and both the initial and current LC yield loci, which are the right intersection between $p-s$ plane and the yield surface in $p-q-s$ space under different suction, are also drawn in Fig. 11 for OCR=10. Since the suction keeps as a constant during cavity expansion under drained condition, the projection of net stress path in $p-s$ plane, is a straight line paralleling to the p −axis, moves rightward from initial stress point O (p_0, s_0) to current stress point F (p_f, s_0). As for the LC yield locus, it expands outward with the cavity expansion as shown in Fig. 11. When suction increases, LC yield locus tends to be perpendicular to the p −axis generally, which means the contribution of suction to unsaturated soil strength is more apparent at lower suction and then reaches a limit value as suction increases.

4.5 Expansion analysis

The curves of expansion-pressure are displayed against the normalized cavity radius a/a_0 for different OCRs and different initial values of suction in Figs. 12 (a) and 12(b), respectively. As the cavity expands gradually, the expansion pressure increases rapidly when the cavity radius is smaller than twice its initial size. However, then it increases much

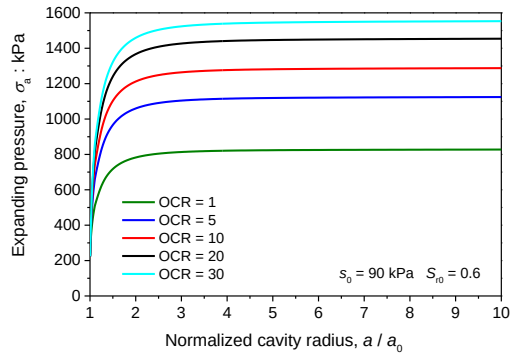

(a)

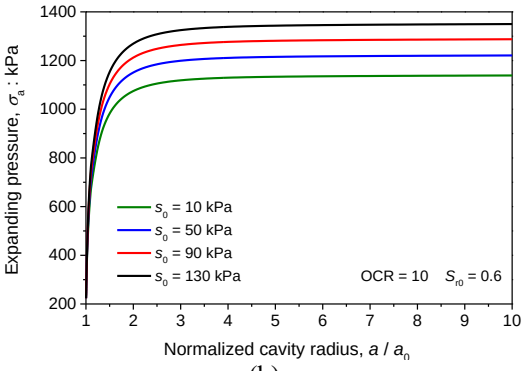

(b)

Fig. 12 Expansion-pressure curves for: (a) different overconsolidation ratios and (b) different initial suction stresses

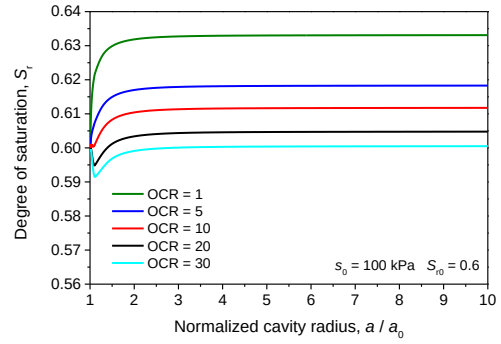

Fig. 13 Variations of degree of saturation at cavity wall with normalized cavity radius for different overconsolidation ratios

more slowly until reaching the limit value of expansion pressure at the instant $a/a_0 = 6$, which indicates that further expansion of the cavity does not require more pressure as the cavity radius is six times its initial value. As anticipated, the expanding pressure is significantly affected by both initial suction and OCR. Under the same OCR, the expansion pressure increases as the initial suction increases, and under the same initial suction, the expansion pressure increases as the OCR significantly increased.

Figs. 13 plots the variation of degree of saturation at cavity wall for different OCRs against the normalized cavity radius a/a_0. As shown in Figs. 13, the degree of saturation changes rapidly in the range $1 < a/a_0 < 2$ and

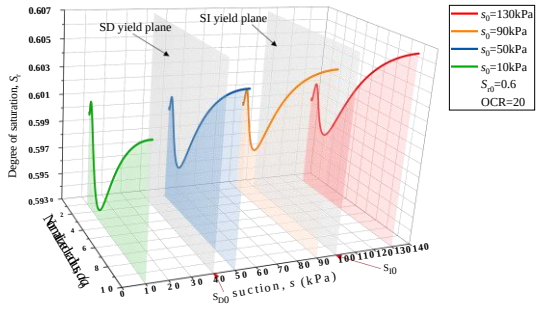

Fig. 14 Evolution of hydraulic parameters at cavity wall in $a/a_0 - s - S_r$ space for OCR=20

reaches a limit value approximately as $a/a_0 = 4$. However, the developing patterns in the range $1 < a/a_0 < 2$ are different with different OCRs. The degree of saturation of NC soil and moderately OC soil increases monotonously while the degree of saturation of OC soil firstly increases a little, then decreases and finally increases to its limit value, which means that OCR has a significant effect on the hydraulic behavior. In addition, the degree of saturation at cavity wall with lower OCR is larger than that with higher OCR during cavity expanding in OC unsaturated soil.

Fig. 14 plots the evolution of degree of saturation and suction at cavity wall in $a/a_0 - s - S_r$ space for OC unsaturated soil with different initial suctions, including 10 kPa, 50 kPa, 90 kPa and 130 kPa. Due to the initial SD and SI yield stresses are 40 kPa and 100 kPa, respectively, the hydraulic state of investigated samples include all three possible positions on SWCC, i.e., located on the wetting curve (with initial suction 10 kPa), scanning curve (with initial suction 50 kPa and 90 kPa) and drying curve (with initial suction 130 kPa). It is shown that the degree of saturation with higher initial suction is higher than that with lower initial suction during cavity expanding in heavily OC unsaturated soil. More importantly, the evolution curves are parallel with SI and SD yield plane, and there is no intersection between evolution curves and SI or SD yield plane. The phenomenon means that no matter what the initial hydraulic state is, whether the hydraulic yield occurs or not will not change during cavity expanding in OC unsaturated soil under drained condition.

5. Conclusions

This study proposed an elastoplastic solution to responses of OC unsaturated soils surrounding an expanding spherical cavity under constant suction condition. The UH model for unsaturated soil and the void-ratio SWCC are combined through the specific volume to model the coupled hydro-mechanical behaviour of OC unsaturated soil around the cavity. The problem analyzed is finally formulated as a set of first-order ordinary differential equations. It can be solved as an initial value problem of four basic unknowns with the help of an auxiliary variable and an iterative algorithm. Parametric studies are carried out to study the distribution of basic unknowns, stress path and the responses on the cavity wall introduced by cavity

expansion.

The results show that the solution proposed herein for spherical cavity expansion in OC unsaturated soil under constant suction condition can reduce to the solution of spherical cavity expanding in saturated soil under drained condition based on the MCC model when both the degree of saturation and OCR equal to 1, which affirms the validation of the proposed solution. Parametric studies reveal three important conclusions: 1) the hydraulic and mechanical behaviors are coupled during cavity expansion in OC unsaturated soil. The existence of suction increases the strength of OC unsaturated soil, and OCR has a substantial influence on distribution of degree of saturation and suction around the spherical cavity; 2) the distribution curves of basic parameters are continuously differentiable along the radial direction, which corresponds to the assumption that the soil yields instantly once the cavity starts to expand and all areas around cavity is elastoplastic based on the UH model for unsaturated soil; 3) the SI yield stress and the SD yield stress remain unchanged during the cavity expansion process under constant suction condition. Hence, whether hydraulic yield will occur or not depends only on the initial relationship among s_{I0}, s_{D0} and s_0.

Acknowledgements

The authors are grateful for the financial support provided by the National Natural Science Foundation of China (Grant No. 41772290) for this research work.

References

Agaiby, S.S. and Mayne, P.W. (2018), "Interpretation of piezocone penetration and dissipation tests in sensitive Leda clay at Gloucester test site", *Can. Geotech. J.*, **55**(12), 1781-1794. https://doi.org/10.1139/cgj-2017-0388.

Alonso, E.E., Gens, A. and Josa, A. (1990), "A constitutive model for partially saturated soils", *Geotechnique*, **40**(3), 405-430. https://doi.org/10.1680/geot.1990.40.3.405.

Bolton, M.D. and Whittle, R.W. (1999), "A non-linear elastic/perfectly plastic analysis for plane strain undrained expansion tests", *Geotechnique*, **49**(1), 133-141. https://doi.org/10.1680/geot.1999.49.1.133.

Carter, J.P., Booker, J.R. and Yeung, S.K. (1986), "Cavity expansion in cohesive frictional soils", *Geotechnique*, **36**(3), 349-358. https://doi.org/10.1680/geot.1986.36.3.349.

Charlez, P.A. and Roatesi, S. (1999), "A fully analytical solution of the wellbore stability problem under undrained conditions using a linearized Cam-Clay model", *Oil Gas Sci. Technol.* **54**(5), 551-563. https://doi.org/10.2516/ogst:1999047.

Chen, H.H. and Mo, P.Q. (2022), "An undrained expansion solution of cylindrical cavity in SANICLAY for K0-consolidated clays", *J. Rock Mech. Geotech. Eng.*, https://doi.org/10.1016/j.jrmge.2021.10.016.

Chen, H.H. and Zhang, L.Y. (2022), "A machine learning-based method for predicting end-bearing capacity of rock-socketed shafts", *Rock Mech. Rock Eng.*, https://doi.org/10.1007/s00603-021-02757-9.

Chen, H.H., Li, L., Li, J.P. and Sun, D.A. (2022), "A generic analytical elastic solution for excavation responses of an arbitrarily-shaped deep opening under biaxial in-situ stresses", *Int. J. Geomech.*, **22**(4), 04022023. https://doi.org/10.1061/(ASCE)GM.1943-5622.0002335.

Chen, S.L. and Abousleiman, Y.N. (2013), "Exact drained solution for cylindrical cavity expansion in modified cam clay soil", *Geotechnique*, **63**(6), 510-517. https://doi.org/10.1680/geot.11.P.088.

Chen, S.L. and Abousleiman, Y.N. (2012), "Exact undrained elasto-plastic solution for cylindrical cavity expansion in modified cam clay soil", *Geotechnique*, **62**(5), 447-456. https://doi.org/10.1680/geot.11.P.027.

Cheng, Y., Yang, H.W. and Sun, D.A. (2018), "Cavity expansion in unsaturated soils of finite radial extent", *Comput. Geotech.*, **102**, 216-228. https://doi.org/10.1016/j.compgeo.2018.06.013.

Collins, I.F., Pender, M.J. and Wang, Y. (1992), "Cavity expansion in sands under drained loading conditions", *Int. J. Numer. Anal. Met.*, **16**(1), 3-23. https://doi.org/10.1002/nag.1610160103.

Collins, I.F. and Stimpson, J.R. (1994), "Similarity solutions for drained and undrained cavity expansions in soils", *Geotechnique*, **44**(1), 21-34. https://doi.org/10.1680/geot.1994.44.1.21.

Cudmani, R. and Osinov, V.A. (2001), "The cavity expansion problem for the interpretation of cone penetration and pressuremeter tests", *Can. Geotech. J.*, **38**(3), 622-638. https://doi.org/10.1139/cgj-38-3-622.

Diao, H.J., Wu, Y.D., Liu, J. and Luo, R.P., (2015), "An analytical investigation of soil disturbance due to sampling penetration", *Geomech. Eng.*, **9**(6), 743-755. https://doi.org/10.12989/gae.2015.9.6.743.

Fahimifar, A., Ghadami, H. and Ahmadvand, M. (2015), "The ground response curve of underwater tunnels, excavated in a strain-softening rock mass", *Geomech. Eng.*, **8**(3), 323-359. https://doi.org/10.12989/gae.2015.8.3.323.

Frydman, S. (2011), "Characterizing the geotechnical properties of natural, Israeli, partially cemented sands", *Geomech. Eng.*, **3**(4), 323-337. https://doi.org/10.12989/gae.2011.3.4.323.

Gong, W.B., Li, J.P., Li, L. and Zhang, S. (2017), "Evolution of mechanical properties of soils subsequent to a pile jacked in natural saturated clays", *Ocean Eng.*, **136**, 209-217. https://doi.org/10.1016/j.oceaneng.2017.03.020.

Gong, W.B., Yang, C.Y., Li, J.P. and Xu, L.C. (2020), "Undrained cylindrical cavity expansion in modified Cam-clay soil: a semi-analytical solution considering biaxial in-situ stresses", *Comput. Geotech.*, **130**, 103888. https://doi.org/10.1016/j.compgeo.2020.103888.

Hoek, E. (2001). "Big tunnels in bad rock." *J. Geotech. Geoenviron. Eng.*, **127**(9), 726–740. https://doi.org/10.1061/(ASCE)1090-0241(2001)127:9(726).

Li, C. and Zou, J.F. (2019), "Created cavity expansion solution in anisotropic and drained condition based on Cam-clay model", *Geomech. Eng.*, **19**(2), 141-151. https://doi.org/10.12989/gae.2019.19.2.141.

Liu, F., Yi, J.T., Cheng, P. and Yao, K. (2020), "Numerical simulation of set-up around shaft of XCC pile in clay", *Geomech. Eng.*, **21**(5), 489-501. https://doi.org/10.12989/gae.2020.21.5.489.

Lukic, D.C., Prokic, A.D. and Brcic, S.V. (2014), "Stress state around cylindrical cavities in transversally isotropic rock mass", *Geomech. Eng.*, **6**(3), 213-233. https://doi.org/gae.2014.6.3.213.

Mayne, P.W. (1991), "Determination of OCR in clays by piezocone tests using cavity expansion and critical state concepts", *Soils Found.*, **31**(2), 65-76. https://doi.org/10.3208/sandf1972.31.2_65.

Palmer A.C. (1972), "Undrained plane-strain expansion of a cylindrical cavity in clay- simple interpretation of pressuremeter test", *Geotechnique*, **22**(3), 451-457.

https://doi.org/10.1680/geot.1972.22.3.451.

Rao, P.P., Chen, Q., Li, L., Nimbalkar, S. and Cui, J. (2017), "Elastoplastic solution for spherical cavity expansion in modified cam-clay soil under drained condition", *Int. J. Geomech.*, **17**(8). https://doi.org/10.1061/(asce)gm.1943-5622.0000925.

Rezania, M., Nezhad, M.M., Zanganeh, H., Castro, J. and Sivasithamparam, N. (2017), "Modeling pile setup in natural clay deposit considering soil anisotropy, structure, and creep effects: case study", *Int. J. Geomech*., **17**(3), 1-13. https://doi.org/10.1061/(ASCE)GM.1943-5622.0000774.

Russell, A.R. and Khalili, N. (2004), "Cavity expansion in unsaturated sands", *Proceedings of the 4th European Congress on Computational Methods in Applied Sciences and Engineering*, Jyvaskyla.

Russell, A.R. and Khalili, N. (2006), "On the problem of cavity expansion in unsaturated soils", *Comput. Mech.*, **37**(4), 311-330. https://doi.org/10.1007/s00466-005-0672-7.

Salgado, R. and Randolph, M.F. (2001), "Analysis of cavity expansion in sand." *Int. J. Geomech.*, **1**(2), 175-192. https://doi.org/10.1061/(ASCE)1532-3641(2001)1:2(175).

Silvestri, V. and Abou-Samra, G. (2012), "Analytical solution for undrained plane strain expansion of a cylindrical cavity in modified cam clay", *Geomech. Eng.*, **4**(1), 19-37. https://doi.org/10.12989/gae.2012.4.1.019.

Sivasithamparam, N. and Castro, J. (2018), "Undrained expansion of a cylindrical cavity in clays with fabric anisotropy: Theoretical solution", *Acta Geotech.*, **13**(3), 729-746. https://doi.org/10.1007/s11440-017-0587-4.

Sun, D.A., Sheng, D.C., Xiang, L. and Sloan, S.W. (2008). "Elastoplastic prediction of hydromechanical behaviour of unsaturated soils under undrained conditions", *Comput. Geotech.*, **35**(6), 845-852. https://doi.org/10.1016/j.compgeo.2008.08.002.

Vrakas, A. (2016), "A rigorous semi-analytical solution for undrained cylindrical cavity expansion in critical state soils", *Int. J. Numer. Anal. Meth. Geomech*., **40**(15), 2137-2160. https://doi.org/10.1002/nag.2529.

Yang, C.Y., Chen, H.H., Li, J.P. and Li, L. (2021), "Undrained spherical cavity expansion in unsaturated soils: Semi-analytical solution coupling hydraulic and mechanical behaviors", *Int. J. Geomech.*, **21**(6), 04021070. https://doi.org/10.1061/(ASCE)GM.1943-5622.0002028.

Yang, C.Y., Li, J.P., Li, L. and Sun, D.A. (2020), "Expansion responses of a cylindrical cavity in overconsolidated unsaturated soils: A semi-analytical elastoplastic solution", *Comput. Geotech.*, **130**. https://doi.org/10.1016/j.compgeo.2020.103922.

Yang, H. and Russell, A.R. (2015), "Cavity expansion in unsaturated soils exhibiting hydraulic hysteresis considering three drainage conditions", *Int. J. Numer. Anal. Met.*, **39**(18), 1975-2016. https://doi.org/10.1002/nag.2379.

Yao, Y.P., Niu, L. and Cui, W.J. (2014), "Unified hardening (UH) model for overconsolidated unsaturated soils", *Can. Geotech. J.*, **51**(7), 810-821. https://doi.org/10.1139/cgj-2013-0183.

Zhang, J.P., Liu, T. and Pei, J.Z. (2020), "Settlement characteristics of bridge approach embankment based on scale model test", *J. Cent. South. Univ. T.*, **27**, 1956-1964. https://doi.org/10.1007 /s11771-020-4422-y.

Zhou, X.Y., He, L.Q. and Sun, D.A. (2022), "Three-dimensional thermal modeling and dimensioning design in the nuclear waste repository", *Int. J. Numer. Anal. Met.*, **46**(4), 779-797. https://doi.org/10.1002/nag.3321.

Zou, J.F., Yang, T., Ling, W., Guo, W.J. and Huang, F.L. (2019), "A numerical stepwise approach for cavity expansion problem in strain-softening rock or soil mass", *Geomech. Eng.*, **18**(3), 225-234. https://doi.org/10.12989/gae.2019.18.3.225.

GC